



A Hybrid Neural Network-Genetic Algorithm Technique for Aircraft Engine Performance Diagnostics

Takahisa Kobayashi
QSS Group, Inc., Brook Park, Ohio

Donald L. Simon
U.S. Army Research Laboratory, Glenn Research Center, Cleveland, Ohio

DISTRIBUTION STATEMENT A
Approved for Public Release
Distribution Unlimited

20010821 055

The NASA STI Program Office . . . in Profile

Since its founding, NASA has been dedicated to the advancement of aeronautics and space science. The NASA Scientific and Technical Information (STI) Program Office plays a key part in helping NASA maintain this important role.

The NASA STI Program Office is operated by Langley Research Center, the Lead Center for NASA's scientific and technical information. The NASA STI Program Office provides access to the NASA STI Database, the largest collection of aeronautical and space science STI in the world. The Program Office is also NASA's institutional mechanism for disseminating the results of its research and development activities. These results are published by NASA in the NASA STI Report Series, which includes the following report types:

- **TECHNICAL PUBLICATION.** Reports of completed research or a major significant phase of research that present the results of NASA programs and include extensive data or theoretical analysis. Includes compilations of significant scientific and technical data and information deemed to be of continuing reference value. NASA's counterpart of peer-reviewed formal professional papers but has less stringent limitations on manuscript length and extent of graphic presentations.
- **TECHNICAL MEMORANDUM.** Scientific and technical findings that are preliminary or of specialized interest, e.g., quick release reports, working papers, and bibliographies that contain minimal annotation. Does not contain extensive analysis.
- **CONTRACTOR REPORT.** Scientific and technical findings by NASA-sponsored contractors and grantees.

- **CONFERENCE PUBLICATION.** Collected papers from scientific and technical conferences, symposia, seminars, or other meetings sponsored or cosponsored by NASA.
- **SPECIAL PUBLICATION.** Scientific, technical, or historical information from NASA programs, projects, and missions, often concerned with subjects having substantial public interest.
- **TECHNICAL TRANSLATION.** English-language translations of foreign scientific and technical material pertinent to NASA's mission.

Specialized services that complement the STI Program Office's diverse offerings include creating custom thesauri, building customized data bases, organizing and publishing research results . . . even providing videos.

For more information about the NASA STI Program Office, see the following:

- Access the NASA STI Program Home Page at <http://www.sti.nasa.gov>
- E-mail your question via the Internet to help@sti.nasa.gov
- Fax your question to the NASA Access Help Desk at 301-621-0134
- Telephone the NASA Access Help Desk at 301-621-0390
- Write to:
NASA Access Help Desk
NASA Center for AeroSpace Information
7121 Standard Drive
Hanover, MD 21076



A Hybrid Neural Network-Genetic Algorithm Technique for Aircraft Engine Performance Diagnostics

Takahisa Kobayashi
QSS Group, Inc., Brook Park, Ohio

Donald L. Simon
U.S. Army Research Laboratory, Glenn Research Center, Cleveland, Ohio

Prepared for the
37th Joint Propulsion Conference and Exhibit
cosponsored by the AIAA, ASME, SAE, and ASEE
Salt Lake City, Utah, July 8–11, 2001

National Aeronautics and
Space Administration

Glenn Research Center

Trade names or manufacturers' names are used in this report for identification only. This usage does not constitute an official endorsement, either expressed or implied, by the National Aeronautics and Space Administration.

Available from

NASA Center for Aerospace Information
7121 Standard Drive
Hanover, MD 21076

National Technical Information Service
5285 Port Royal Road
Springfield, VA 22100

Available electronically at <http://gltrs.grc.nasa.gov/GLTRS>

A HYBRID NEURAL NETWORK-GENETIC ALGORITHM TECHNIQUE FOR AIRCRAFT ENGINE PERFORMANCE DIAGNOSTICS

Takahisa Kobayashi*
QSS Group, Inc.
Brook Park, Ohio 44142

Donald L. Simon†
U.S. Army Research Laboratory
NASA Glenn Research Center
Cleveland, Ohio 44135

Abstract

In this paper, a model-based diagnostic method, which utilizes Neural Networks and Genetic Algorithms, is investigated. Neural networks are applied to estimate the engine internal health, and Genetic Algorithms are applied for sensor bias detection and estimation. This hybrid approach takes advantage of the nonlinear estimation capability provided by neural networks while improving the robustness to measurement uncertainty through the application of Genetic Algorithms. The hybrid diagnostic technique also has the ability to rank multiple potential solutions for a given set of anomalous sensor measurements in order to reduce false alarms and missed detections. The performance of the hybrid diagnostic technique is evaluated through some case studies derived from a turbofan engine simulation. The results show this approach is promising for reliable diagnostics of aircraft engines.

Nomenclature

| | |
|-----|---------------------------|
| A8 | Nozzle area |
| A16 | Variable bypass duct area |
| BST | Booster |
| CLM | Component Level Model |
| FAN | Fan |
| GA | Genetic Algorithms |
| HPC | High-Pressure Compressor |
| HPT | High-Pressure Turbine |
| LPC | Low-Pressure Compressor |

* Aerospace Engineer

† Electronics Engineer, Member

Copyright © 2001 by the American Institute of Aeronautics and Astronautics, Inc. No copyright is asserted in the United States under Title 17, U.S. Code. The U.S. Government has a royalty-free license to exercise all rights under the copyright claimed herein for Governmental Purposes. All other rights are reserved by the copyright owner.

| | |
|------|---------------------------------|
| LPT | Low-Pressure Turbine |
| MBD | Model Based Diagnostics |
| N2 | Low pressure spool speed |
| N25 | High pressure spool speed |
| P27D | Booster tip pressure |
| P42 | Inter-turbine pressure |
| PS15 | Bypass duct static pressure |
| PS21 | Fan exit static pressure |
| PS3 | Combustor inlet static pressure |
| T27 | HPC inlet temperature |
| T3 | Combustor inlet temperature |
| WF36 | Fuel Flow |

Introduction

Over the last several decades, significant research efforts have been directed at the development of performance diagnostic systems for aircraft engines. Such systems can provide a variety of benefits to aircraft operators including improved safety,¹ improved reliability, and reduced operating costs. With the significant growth in air traffic projected in the coming years, it is expected that the demand for enhanced performance diagnostic methods will continue to increase.

In this work, aircraft engine performance diagnostics is accomplished by estimating a set of internal engine health parameters from available sensor measurements. These measurements, which include gas path temperatures and pressures, spool speeds, fuel flows, and variable geometry, provide information regarding the health of the engine. The general approach to performance diagnostics can be expressed using the following relationship between the engine health parameters and the sensed parameters.

$$y = f(p, \text{operating condition}) + w \quad (1)$$

where y is an $m \times 1$ vector representing sensed parameters, p is an $n \times 1$ vector of engine health parameter deltas (deviations from nominal), $f(\cdot)$ is a nonlinear function of p and operating condition such as altitude and engine power level, and w is an $m \times 1$ vector representing measurement inaccuracies including bias and white noise. The problem is to estimate the health parameter delta vector p given the sensed parameter vector y .

Several issues make this problem highly challenging. First, the only information available for health parameter estimation is the sensed parameters, and the number of health parameters to be estimated is often greater than the number of sensors available. For such an underdetermined problem, there exists an infinite number of solutions for a given set of sensor measurements, and some assumptions must be made to select the best or most probable solution. One option is to assume that the most likely solution has the minimum deviation from the condition estimated in the previous time frame assuming the health condition is expected to degrade gradually rather than rapidly. A second issue is that accurate estimation of health parameters may not be achieved if sensor locations are not appropriate. For instance, assume that a health parameter is primarily affecting the flow condition in the bypass duct and has a minor influence on the core flow. It will be difficult to estimate this health parameter from core flow measurements alone even if there are an excessive number of sensors. In such a case, some health parameters are unobservable since critical measurements are missing. Another issue is that the sensor measurements are often distorted by noise and bias as described in Equation 1, thereby masking the true condition of the engine and leading to incorrect estimation results. Moreover, accurate statistical information to characterize measurement uncertainty may not be available, and filtering techniques are ineffective against biases. Sensor biases are often treated as part of the engine health parameters because of their relatively large magnitude and time-invariant character. However, this obviously increases the number of unknowns in the estimation problem. Finally, the combined effect of system non-linearity and sensor selection may result in multiple health degradation scenarios producing similar measurement shifts. This is a difficult problem to deal with because estimation techniques, in general, give only one set of estimated health parameters for a given set of measurements without the capability to indicate the level of confidence in the results. One possible approach which addresses this issue involves the use of a failure data base developed *a priori* from flight tests or simulation; several possible solutions are selected from the data base and a confidence level is determined

using statistical approaches. Incorporation of intelligence in the estimation architecture is indispensable in determining the most reasonable solution in the highly nonlinear and noise-corrupted problem environment. A health monitoring system without the capability to deal with these issues will exhibit unacceptable false alarm or missed detection rates.

Researchers have investigated a number of estimation techniques such as Weighted Least-Squares,^{2,3} Kalman Filters,^{4,5,6} Neural Networks,^{7,8} and Genetic Algorithms.^{9,10} Each approach has relative strengths, however, a technique that is capable of addressing all of the above issues has not yet emerged. In this paper, the engine diagnostics problem is approached through a Model-Based Diagnostic method utilizing Neural Networks and Genetic Algorithms. The proposed technique takes advantage of the nonlinear estimation capability provided by neural networks while improving the robustness to measurement uncertainty due to bias through the application of Genetic Algorithms. The hybrid diagnostic technique also has the capability to rank multiple potential solutions for a given set of anomalous sensor measurements in order to reduce false alarms and missed detections.

Model-Based Diagnostics

One approach to aircraft engine performance diagnostics that has been investigated by a number of researchers is called Model-Based Diagnostics (MBD).^{2-6,8-12} As shown in Figure 1, the MBD architecture is composed of an engine model and an associated parameter estimation algorithm for monitoring engine component performance deterioration. The engine model can be linear or nonlinear. In this architecture, a set of engine model

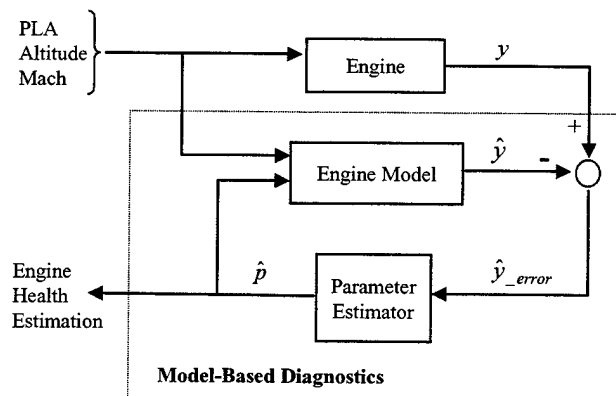


Figure 1. Model-Based Diagnostics Architecture.

health parameters, \hat{p} , is tuned such that the model outputs match the engine physical sensor measurements. It is assumed that the health parameters have sufficient authority to describe the actual engine's performance variations due to component degradations. In addition to estimated health parameters, an accurately tuned engine model provides estimated sensor values as well as estimations of unmeasurable parameters such as thrust and component stall margins. With these estimated parameters, a variety of accommodating actions can be performed to prevent the progression of damage. Estimated health parameter information can be integrated with control system logic in the development of a comprehensive engine health management system which maintains safe operation of the propulsion system by simultaneously considering performance and engine operability.

Engine Model

In this research, the XTE46 engine model developed by General Electric Aircraft Engines (GEAE)¹² was used. This model is constructed as a Component Level Model (CLM), which assembles the major components of an aircraft engine. The CLM is a nonlinear simulation that represents engine physics and is capable of real-time execution. The XTE46 engine model is a scaled, unclassified representation of an advanced military twin-spool turbofan engine. Engine performance deterioration is modeled by adjustments to efficiency and/or flow coefficient scalars of the following components: Fan (FAN), Booster (BST), High-Pressure Compressor (HPC), High-Pressure Turbine (HPT), and Low-Pressure Turbine (LPT). A set of nine health parameters, shown in Table 1, must be estimated correctly in order to diagnose the engine health condition. There are 17 sensors and three actuators that

can potentially be used as sensed parameters. In a realistic application, such a large set of sensors would not be available. After some investigation, a set of 12 sensed parameters was selected as shown in Table 1. In the current study, the performance of the health estimator is evaluated in the simulation environment. The XTE46 CLM is used to represent both the physical engine and the MBD system engine model.

Nonlinear Effects of Health Degradation

One of the challenges often encountered in the health estimation problem is the highly nonlinear relation between health parameters and sensed parameters. It is possible that small degradations in health parameters, which are considered insignificant from an operability perspective, can cause large shifts in the sensor measurements. Likewise, significant degradation in a single health parameter can result in small measurement shifts relative to the standard noise level. Furthermore, there is a chance that distinct health degradations will result in indistinguishable shifts in sensor measurements.¹¹ An example of this is shown in Figure 2 which compares the measurement shifts for two health degradation scenarios at cruise condition: Case A for 2% degradations in Fan and LPT efficiencies, and Case B for a 3% degradation in Fan efficiency. The two cases are distinct, however, the differences in all sensor measurements between these two cases are within the range of noise. One approach to address this problem is to incorporate some intelligence logic which can provide a list of possible degradation scenarios for given measurement shifts. Even if a diagnostic system cannot give a clear answer, such a list can provide very useful information to maintenance personnel attempting to troubleshoot anomalous engine behavior. Another

Table 1. XTE46 Engine Variables

| Health Parameter | | Sensed Parameter | |
|------------------|----------------|------------------|------|
| 1 | FAN efficiency | 1 | N2 |
| 2 | FAN flow | 2 | N25 |
| 3 | BST flow | 3 | T27 |
| 4 | HPC efficiency | 4 | T3 |
| 5 | HPC flow | 5 | PS15 |
| 6 | HPT efficiency | 6 | PS21 |
| 7 | HPT flow | 7 | P27D |
| 8 | LPT efficiency | 8 | PS3 |
| 9 | LPT flow | 9 | P42 |
| | | 10 | WF36 |
| | | 11 | A8 |
| | | 12 | A16 |

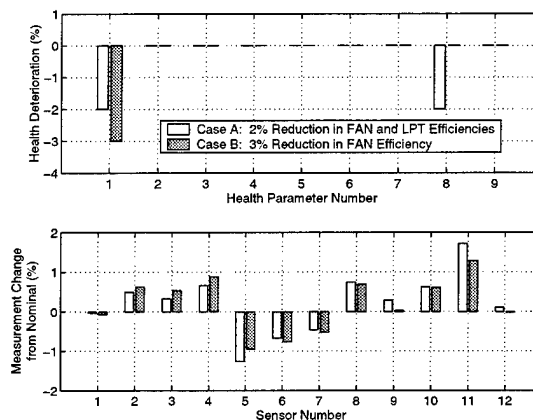


Figure 2. Comparison of Two Degradation Cases at Cruise Condition.

approach is to use sensor measurements from more than one operating point so that a unique set of measurement shifts can be assigned for each degradation scenario. This approach takes advantage of the non-linearity in the system. Diagnostics based on multiple operating points^{10,13} has been investigated by several researchers, but it has some limitations. First, it must be assumed that a given health degradation does not progress as multiple operating points are traversed. Second, it takes additional time to reach a diagnosis. Third, additional restrictions may be imposed on the selection of diagnostic sensors. In the current research, feedback parameters regulated by a control system must be excluded from the diagnostic sensor suite since bias in a feedback parameter causes other sensor measurements to shift. In such a case where a bias has a health-degradation-like effect on multiple sensors, the nonlinear function in Equation 1 becomes a function of that bias in addition to health parameters and operating condition. This obviously increases the number of unknown parameters in the problem. Since different parameters may be regulated at different operating points due to control mode changes, the number of diagnostic sensors which can be used across multiple operating points is limited. As the number of operating points increases, the impact of the above three issues increases, and a multi-point diagnostic approach becomes less practical.

Hybrid Neural Network-Genetic Algorithm Estimation Architecture

Accurately estimating the health parameters is a critical issue for the development of a MBD system. Any estimation architecture must be able to handle non-linearity as well as be robust to sensor noise and bias as discussed earlier.

The estimation architecture in this paper combines neural networks and Genetic Algorithms (GA) for aircraft engine performance diagnostics at steady-state conditions. It is assumed that the sensor measurements are time averaged; however, they still contain some uncertainty due to sensor noise and modeling errors. Neural networks exhibit excellent nonlinear estimation capabilities, but the training set required to fully represent all possible permutations of health parameters and sensor bias is prohibitively large. It would take excessive time to train such neural networks, and their performance might not reach a satisfactory level. In order to avoid this problem, the approach taken by the hybrid estimator designates neural networks for the health estimation task while designating GA for the sensor bias detection task. This approach reduces the size of the training set significantly.

The problem setup is shown in Figure 3. The vector p represents a set of health parameter deltas to be estimated. In the simulation environment, the measurement uncertainty vector in Equation 1 is decomposed as

$$w = b + v \quad (2)$$

where b and v represent a bias vector and a white noise vector, respectively. In this paper, it is assumed that at most one sensor can be biased at a time to make the problem manageable. Thus, the bias vector contains one non-zero value at most, and its magnitude must be large relative to the expected noise magnitude. This vector will be estimated; however, the estimated value of the non-zero element will be under the influence of noise to some degree since bias and noise contained in measurements are indistinguishable. Therefore, an estimated bias vector will have only one non-zero value, just as the actual bias vector b does, but the estimated value will be an approximation of the largest normalized value contained in the uncertainty vector w . The unknown vectors p and b must be estimated based on the available physical sensor measurements y .

As shown in the figure, the hybrid estimator architecture is composed of the bias data set, the neural network estimator, the engine model, and the GA optimization technique. The bias data set, which is composed of a large number of bias vectors, is defined *a priori* and is used by the GA in the search for a bias vector that matches well with an actual bias contained in the measurement vector. The neural network estimator is trained off-line with noise-corrupted but bias-free sensor measurements, and it will perform sufficiently well in estimating health parameters as long as the sensor measurements do not contain any bias. For a given set of estimated health parameters and sensor bias, the engine model is executed and its outputs are evaluated against the physical sensor measurements. The bias data set, the neural network estimator, and the engine model are coordinated by the GA in the search for an optimal solution.

Bias Data Set

The bias data set defines the solution space over which the GA searches for an optimal sensor bias solution. It is composed of a set of bias vectors, each of which has a non-zero value only in the k^{th} entry, defining the bias value and also identifying the k^{th} sensor as biased. A vector with zeros in all entries is also included in the data set to account for the case where no bias is present. The bias values for each sensor are equally spaced, based on the noise standard deviation σ over a range of possible values. The minimum bias value is defined by

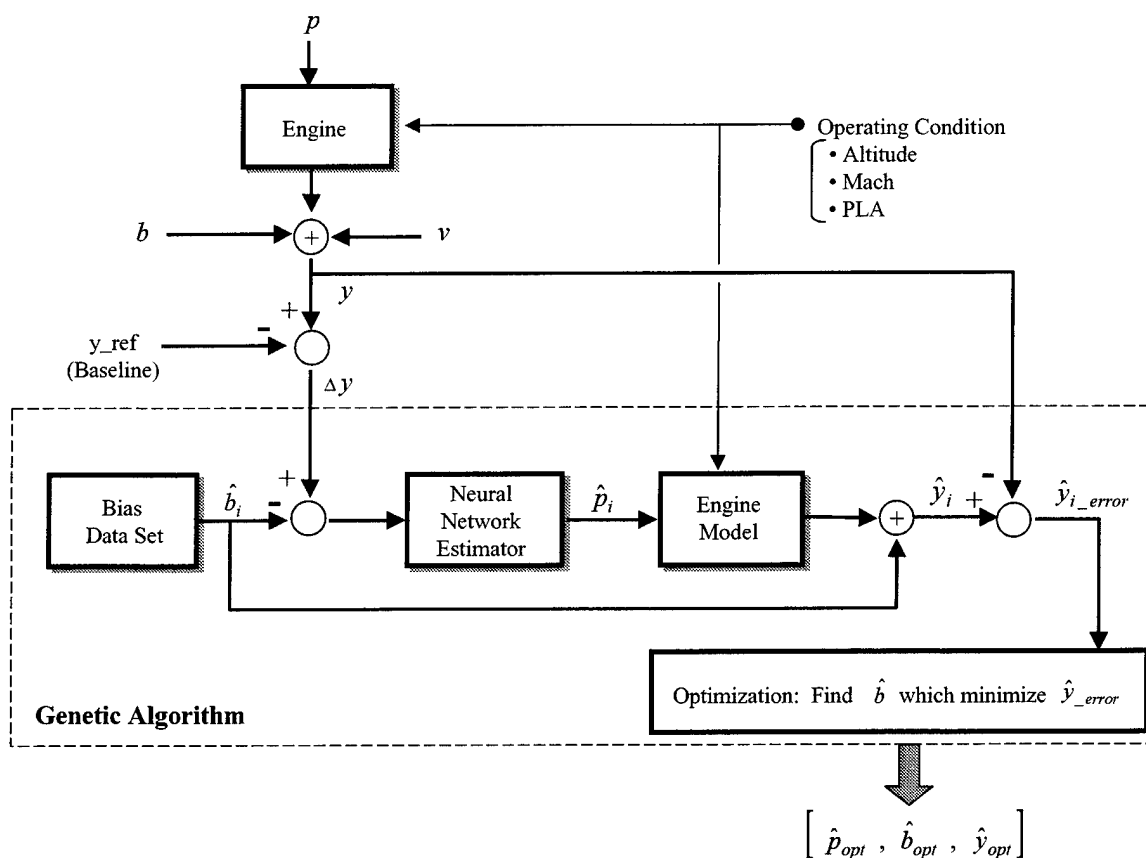


Figure 3. Hybrid Engine Health Estimation Architecture.

the detection threshold while the maximum value is set in accordance with a bound that would typically disqualify the sensor for being out of range, as shown in Figure 4. The detection threshold is set large enough so that noise is unlikely to be interpreted as a bias. In this paper, the threshold is set to 4σ while the upper bound is set to 20σ .

Neural Network Estimator Design

The neural network estimator is the key element of the hybrid architecture. As mentioned earlier, the neural network estimator does not need to account for sensor bias, but it still has to tolerate the effects of measurement uncertainty due to noise. The robustness of the estimator can be improved by using noise-corrupted sensor measurements during training so that neural networks will learn to distinguish the range of measurement shifts due to noise and those due to health degradations. However, since the number of health degradation scenarios that an engine may encounter is

virtually infinite, it is still a challenging problem to develop an estimator that performs adequately well. It was found that sensor measurements from at least two operating points were needed in order to achieve the desired estimation performance level. This problem may be due to sensor location, sensor noise, highly nonlinear engine dynamics, or a combination of these as discussed earlier. Table 2 compares the performance of two estimators; one designed at cruise condition and another designed using data from cruise and takeoff conditions. For the two-point design, the estimation process is initiated after the steady-state data at the second operating point are collected. Both of them are composed from nine multiple-input, single-output sub-estimators, each of which was developed using a feedforward neural network. They were trained by backpropagation using about 3000 degraded engines. The single-point design has 12 inputs while the two-point design has 24 inputs. The table shows the standard deviation and mean value of estimation errors. The result was obtained using the sensor measurements

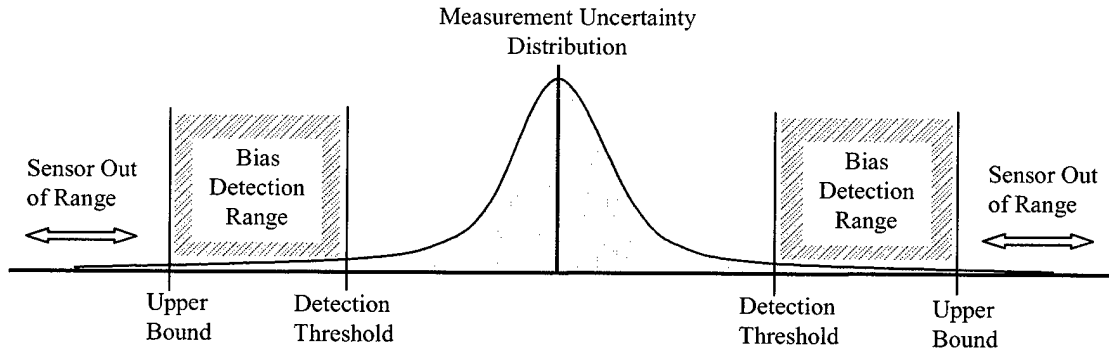


Figure 4. Measurement Uncertainty Distribution with Bias Detection Thresholds.

of 500 degraded engines without noise. These 500 engines were not used in the neural network training. Although a single-point diagnostic approach is desired as discussed earlier, it was found to provide unsatisfactory estimation accuracy. Thus a multi-point estimator is utilized. It should be noted that some of the health parameters are more difficult to accurately estimate than others.

Table 2. Performance Comparison of Estimators

| | Single-Point Design at Cruise | | Two-Point Design at Cruise & Takeoff | |
|-------------|----------------------------------|--|---|--|
| | Mean Absolute Error (%) | Standard Deviation of % Error | Mean Absolute Error (%) | Standard Deviation of % Error |
| FAN Eff | 9.00 | 13.01 | 5.55 | 9.15 |
| FAN Flow | 5.42 | 9.28 | 2.92 | 4.77 |
| BST Flow | 6.08 | 9.90 | 5.03 | 8.55 |
| HPC Eff | 9.64 | 15.22 | 4.19 | 7.79 |
| HPC Flow | 9.39 | 15.69 | 5.52 | 9.30 |
| HPT Eff | 8.86 | 14.66 | 4.91 | 8.50 |
| HPT Flow | 2.94 | 4.92 | 1.51 | 2.65 |
| LPT Eff | 10.33 | 15.16 | 6.38 | 10.09 |
| LPT Flow | 5.63 | 9.11 | 2.79 | 4.70 |

Genetic Algorithm Optimization Process

To find an optimal solution in the bias data set, the GA search sequence shown in Figure 3 proceeds as follows.

First, a bias vector \hat{b}_i selected from the bias data set is subtracted from physical sensor measurement deltas (the deviations from nominal condition) Δy , and the resultant vector is fed into the neural network estimator. If the selected bias vector is identical or close to the true bias b , then the bias in the measurements is cancelled out. This allows the neural network estimator to generate an accurate estimation of the health parameter vector \hat{p}_i from the bias-free measurements.

The engine model is run with inputs of \hat{b}_i and \hat{p}_i to synthesize engine sensor outputs \hat{y}_i for comparison with the sensor measurements.

For each selected bias vector \hat{b}_i , the following cost function, which accounts for the multi-point estimator, is computed.

$$J_i = \left(\sum_{j=1}^m \left[\frac{(\hat{y}_i)_j - y_j}{W_j} \right]^2 \right)_{Cruise} + \sum_{j=1}^m \left[\frac{(\hat{y}_i)_j - y_j}{W_j} \right]^2 \bigg|_{Takeoff} \right)^{1/2} \quad (3)$$

where m is the number of sensors and

$$W_j = \begin{cases} \sigma_j & \text{when } j = k \\ 3\sigma_j & \text{otherwise} \end{cases} \quad (4)$$

where σ_j is a standard deviation of noise in sensor j , and k indicates the non-zero entry of a selected bias vector. The parameter W_j normalizes the estimation error while imposing a larger penalty for discrepancies in the k^{th}

sensor. If a selected bias vector contains a bias estimation value in the wrong sensor, the estimation error in the k^{th} entry is magnified. The noise standard deviation for the sensors changes with operating point. Therefore, in the above equation, W_j and noise contained in y_j are based on the corresponding sensor σ values at the specific operating point. However, the σ value used to create bias intervals in the bias data set is based on the σ value at the cruise condition.

A value indicating the estimation accuracy, or fitness value, for each selected bias vector is defined as

$$\text{Fitness}_i = K/J_i \quad (5)$$

where K is a constant for normalization. In this paper, a fitness value larger than 1 indicates good agreement between model outputs and actual measurements. The fitness value becomes larger as the output error between \hat{y}_i and y_i diminishes.

A unique aspect of the GA search process is that a set of multiple points in the solution space is evaluated at each iteration, and the content of this set is updated from iteration to iteration. In the GA problem setup, each bias vector in the data set is referred to as an "individual," and a number of individuals are selected from the data set to construct a "population." At each iteration, or "generation," the entire population is evaluated, and a fitness value is assigned to each individual. The higher the fitness value, the higher the probability that the corresponding individual will survive into the next generation. The population of the next generation is constructed from individuals of the previous generation and individuals newly introduced from the data set. As the population is updated from generation to generation, those individuals with high fitness values will occupy the major portion of the population. The objective of the GA optimization is to find the best individual among the data set through this search process. Unlike gradient search methods, the GA search process starts from multiple points set by the initial population; this helps to avoid convergence to a local peak in the highly nonlinear environment. Moreover, the fitness values indicate the level of confidence in the estimation. If an appropriate estimation set is not found in the search process, the fitness value will remain small. This indicates the best estimation set should not be relied upon for accurate diagnosis of engine health although an anomalous condition may exist.

A GA is generally run for many generations until the set of individuals constructing the population converges to a single individual. In the current study, the GA is

run for relatively few generations. In this highly nonlinear and noisy environment, it is possible to have dissimilar faults producing similar sensor signatures, as was illustrated in Figure 2. Running the GA until convergence to a single individual can lead to erroneous conclusions regarding engine health. After the search process, the searched bias vectors are ranked based on their corresponding fitness values. A list of several fault candidates can help to avoid false alarms or missed detections. Moreover, running the GA for fewer generations can save a significant amount of computing time.

Results of Hybrid Estimator Performance

This section shows some of the results obtained from an extensive assessment of the hybrid estimator. Table 3 shows the estimation of health parameters from sensor measurements which contain no bias. The set of actual health parameters shown in Table 3 was not a part of the neural network estimator training set. There are no clear guidelines to define the adequate performance

Table 3. Health Parameter Estimation Without Sensor Bias

| Health Parameter | Actual Condition (%) | Estimated Condition (%) | % Error $(\hat{p} - p)/p * 100$ |
|------------------|----------------------|-------------------------|---------------------------------|
| FAN Eff | -2.900 | -2.793 | -3.682 |
| FAN Flow | -1.800 | -1.819 | 1.029 |
| BST Flow | 0.000 | 0.000 | ----- |
| HPC Eff | -2.300 | -2.177 | -5.367 |
| HPC Flow | -1.900 | -2.016 | 6.078 |
| HPT Eff | -1.400 | -1.612 | 15.138 |
| HPT Flow | 1.000 | 0.883 | -11.750 |
| LPT Eff | -2.000 | -2.199 | 9.930 |
| LPT Flow | 2.100 | 2.093 | -0.320 |

| Sensor | Normalized Estimation Error $(\hat{y} - y)/3\sigma$ | |
|--------|---|---------|
| | Cruise | Takeoff |
| N2 | 0.750 | -0.069 |
| N25 | -0.155 | 0.755 |
| T27 | -0.378 | 0.007 |
| T3 | 0.482 | 0.028 |
| PS15 | 0.146 | 0.029 |
| PS21 | -0.059 | 0.163 |
| P27D | 0.281 | 0.600 |
| PS3 | 0.155 | 1.095 |
| P42 | -0.235 | 0.467 |
| WF36 | -0.222 | 0.412 |
| A8 | 0.198 | 0.121 |
| A16 | -0.263 | -0.062 |

level in the highly nonlinear environment of the current study. In this paper, the performance of the estimator is considered satisfactory if the maximum health estimation error is less than 30%. Table 3 shows both good sensor matching and good health estimation accuracy, meeting with the performance requirements. It should be noted that estimation accuracy is influenced by sensor noise.

When one of the sensors is biased, the neural network estimator alone can no longer accurately estimate health parameters. The following example shows a case where the fuel flow sensor has a 9.5σ bias with the same health degradation as shown in Table 3. This bias magnitude is in the medium range of the current problem setup. After the GA search process, the hybrid estimator provides the rank of bias estimations as shown in Table 4 and the corresponding plots shown in Figure 5. Table 4 shows the identification numbers of biased sensors, bias values, and corresponding fitness values. Sensor matching is considered adequate if the fitness value is larger than 0.75 and is considered very good if the fitness value is larger than 1. Therefore, the top four bias estimations are good candidates for representing the actual bias. Figure 5 shows the fitness values of individuals (bias vectors) selected by the GA during the search process. The horizontal axis varies from -20σ to 20σ with a 1σ increment. The bias vector representing the no-bias case is shown at the center of all plots, providing a baseline for comparison between estimations with and without bias detection. As mentioned earlier, the detection threshold is set to 4σ . The bias data set contains 409 individuals and the population size is set to 50. The initial population included four individuals from each sensor, two individuals for each bias direction.

Table 4. Rank of Sensor Bias Estimation After the GA Search (Case 1: 9.5σ Bias in WF36)

| Rank | Sensor ID | Bias Value (σ) | Fitness |
|------|-----------|-------------------------|---------|
| 1 | 10 (WF36) | 10 | 1.036 |
| 2 | 10 (WF36) | 9 | 1.020 |
| 3 | 10 (WF36) | 11 | 0.878 |
| 4 | 10 (WF36) | 8 | 0.852 |
| 5 | 10 (WF36) | 7 | 0.723 |
| 6 | 10 (WF36) | 12 | 0.594 |
| 7 | 10 (WF36) | 6 | 0.554 |
| 8 | 10 (WF36) | 13 | 0.512 |
| 9 | 10 (WF36) | 5 | 0.458 |
| 10 | 10 (WF36) | 14 | 0.402 |

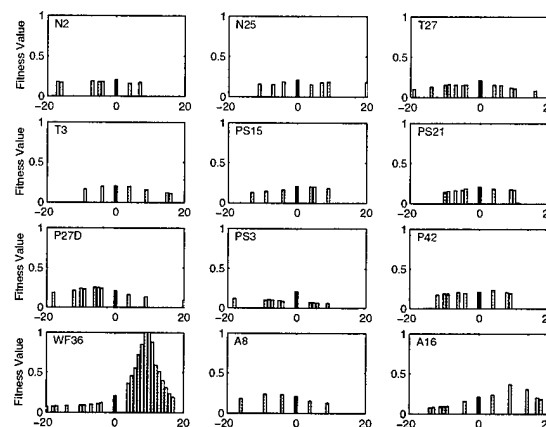


Figure 5. Fitness Values of Individuals Selected by GA Search. (Case 1: 9.5σ Bias in WF36)

Table 5 shows the health parameter estimation and sensor matching of the estimator with and without bias detection. The estimation result of the individual ranked first in Table 4 is shown. For the estimator with bias detection, the performance requirement is met. Although the estimation errors of HPT efficiency and HPT flow coefficient are relatively high among the health parameters, a similar trend was noticed in the previous example where no bias was present, as was shown in Table 3. This illustrates the highly effective performance of the hybrid estimator in isolating a sensor bias.

The task of bias detection and estimation becomes easier for larger biases. With a large bias in the measurements, the cost function value of Equation 3 ideally remains large unless the bias is canceled out by an accurate estimate. This task becomes more difficult for small biases which are less distinguishable from noise. Table 6, Figure 6, and Table 7 show a case where the fuel flow sensor has a 4.5σ bias with the same health degradation as shown in Table 3. Table 6 and Figure 6 show that the individuals representing the bias in the correct sensor (WF36) no longer dominate the GA population as they did in the previous case with a larger bias value. Depending on the sensor noise profile, this ranking can change, and the correct sensor may not be ranked highest. The performance goal of the hybrid estimator is to at least capture the correct sensor in the ranking of plausible solutions in order to avoid missed detection. For smaller bias magnitudes, the robustness of the neural network estimator is demonstrated. The bias vector representing the no-bias case (Sensor ID 0) is ranked 4th overall, and the corresponding health estimations and sensor matching shown in Table 7 are well within the acceptable range.

**Table 5. Health Parameter Estimation With and Without Bias Detection
(Case 1: 9.5 σ Bias in WF36)**

| Health Parameter | Actual Condition (%) | With Bias Detection | | Without Bias Detection | |
|------------------|----------------------|-------------------------|---------|-------------------------|---------|
| | | Estimated Condition (%) | % Error | Estimated Condition (%) | % Error |
| FAN Efficiency | -2.900 | -2.788 | -3.876 | -2.950 | 1.722 |
| FAN Flow | -1.800 | -1.811 | 0.596 | -1.819 | 1.076 |
| BST Flow | 0.000 | 0.000 | ----- | -0.134 | ----- |
| HPC Efficiency | -2.300 | -2.172 | -5.578 | -2.305 | 0.234 |
| HPC Flow | -1.900 | -2.027 | 6.658 | -1.497 | -21.213 |
| HPT Efficiency | -1.400 | -1.614 | 15.254 | -1.715 | 22.516 |
| HPT Flow | 1.000 | 0.875 | -12.484 | 2.201 | 120.045 |
| LPT Efficiency | -2.000 | -2.197 | 9.857 | -2.303 | 15.146 |
| LPT Flow | 2.100 | 2.083 | -0.819 | 2.393 | 13.942 |

| | | With Bias Detection | | | Without Bias Detection | |
|--------|--------------|-----------------------------|--------|---------|-----------------------------|---------|
| | | Error $(\hat{y}-y)/3\sigma$ | | | Error $(\hat{y}-y)/3\sigma$ | |
| Sensor | Actual Bias | Estimated Bias | Cruise | Takeoff | Cruise | Takeoff |
| N2 | 0 | 0 | 0.751 | -0.070 | 3.432 | -0.109 |
| N25 | 0 | 0 | -0.154 | 0.754 | -1.896 | -0.352 |
| T27 | 0 | 0 | -0.377 | 0.006 | 0.453 | 0.078 |
| T3 | 0 | 0 | 0.482 | 0.027 | 0.204 | -0.275 |
| PS15 | 0 | 0 | 0.146 | 0.030 | -1.439 | -0.369 |
| PS21 | 0 | 0 | -0.058 | 0.163 | 0.767 | 0.100 |
| P27D | 0 | 0 | 0.281 | 0.600 | 1.217 | 0.543 |
| PS3 | 0 | 0 | 0.157 | 1.091 | -3.064 | -10.008 |
| P42 | 0 | 0 | -0.234 | 0.466 | -0.561 | 0.194 |
| WF36 | 9.5 σ | 10 σ | -0.055 | 0.490 | -2.906 | -0.645 |
| A8 | 0 | 0 | 0.198 | 0.120 | 2.313 | 0.397 |
| A16 | 0 | 0 | -0.263 | -0.063 | 0.159 | -0.488 |

Table 6. Rank of Sensor Bias Estimation for Small Bias (Case 2: 4.5 σ Bias in WF36)

| Rank | Sensor ID | Bias Value (σ) | Fitness |
|------|-------------|-------------------------|---------|
| 1 | 10 (WF36) | 5 | 1.035 |
| 2 | 10 (WF36) | 4 | 1.022 |
| 3 | 10 (WF36) | 6 | 0.878 |
| 4 | 0 (No bias) | 0 | 0.863 |
| 5 | 9 (P42) | 4 | 0.828 |
| 6 | 12 (A16) | 4 | 0.813 |
| 7 | 12 (A16) | 5 | 0.776 |
| 8 | 11 (A8) | -4 | 0.776 |
| 9 | 9 (P42) | 5 | 0.765 |
| 10 | 12 (A16) | 6 | 0.757 |

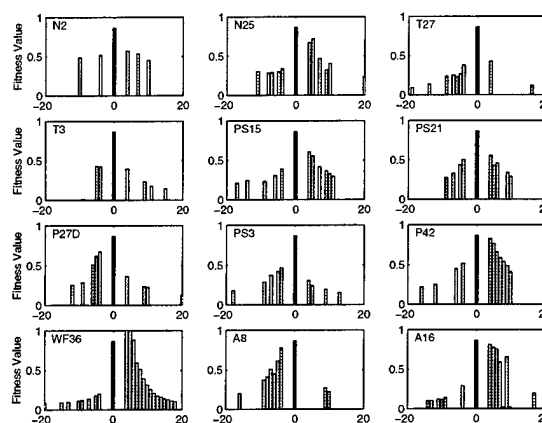


Figure 6. Fitness Values of Individuals Selected by GA Search. (Case 2: 4.5 σ Bias in WF36)

**Table 7. Health Parameter Estimation With and Without Bias Detection
(Case 2: 4.5σ Bias in WF36)**

| | | With Bias Detection | | Without Bias Detection | |
|------------------|----------------------|-------------------------|---------|-------------------------|---------|
| Health Parameter | Actual Condition (%) | Estimated Condition (%) | % Error | Estimated Condition (%) | % Error |
| FAN Efficiency | -2.900 | -2.787 | -3.887 | -2.865 | -1.224 |
| FAN Flow | -1.800 | -1.810 | 0.538 | -1.864 | 3.557 |
| BST Flow | 0.000 | 0.000 | ----- | 0.000 | ----- |
| HPC Efficiency | -2.300 | -2.175 | -5.456 | -2.228 | -3.137 |
| HPC Flow | -1.900 | -2.026 | 6.624 | -1.881 | -1.018 |
| HPT Efficiency | -1.400 | -1.608 | 14.876 | -1.642 | 17.259 |
| HPT Flow | 1.000 | 0.877 | -12.310 | 1.235 | 23.506 |
| LPT Efficiency | -2.000 | -2.197 | 9.824 | -2.227 | 11.330 |
| LPT Flow | 2.100 | 2.085 | -0.706 | 2.220 | 5.723 |

| | | With Bias Detection | | | Without Bias Detection | |
|--------|-------------|---------------------|-------------------------------|---------|-------------------------------|---------|
| | | Estimated Bias | Error $(\hat{y} - y)/3\sigma$ | | Error $(\hat{y} - y)/3\sigma$ | |
| Sensor | Actual Bias | Estimated Bias | Cruise | Takeoff | Cruise | Takeoff |
| N2 | 0 | 0 | 0.759 | -0.070 | 1.237 | -0.021 |
| N25 | 0 | 0 | -0.149 | 0.754 | -0.365 | 0.674 |
| T27 | 0 | 0 | -0.376 | 0.006 | -0.256 | -0.002 |
| T3 | 0 | 0 | 0.483 | 0.027 | 0.409 | -0.044 |
| PS15 | 0 | 0 | 0.144 | 0.029 | -0.075 | 0.057 |
| PS21 | 0 | 0 | -0.057 | 0.162 | -0.014 | -0.115 |
| P27D | 0 | 0 | 0.283 | 0.600 | 0.316 | 0.278 |
| PS3 | 0 | 0 | 0.161 | 1.093 | -0.593 | -1.506 |
| P42 | 0 | 0 | -0.232 | 0.466 | -0.362 | 0.260 |
| WF36 | 4.5σ | 5σ | -0.052 | 0.489 | -1.617 | -0.198 |
| A8 | 0 | 0 | 0.203 | 0.120 | 0.497 | 0.117 |
| A16 | 0 | 0 | -0.260 | -0.063 | -0.269 | -0.201 |

Concluding Remarks

A hybrid estimation technique for aircraft engine performance diagnostics was presented in this paper. The hybrid architecture consists of Neural Networks and Genetic Algorithms, which function synergistically for estimating health parameters from biased sensor measurements. Neural networks are well suited for estimating health parameters in a highly nonlinear environment. However, a major problem arises when the size of training data set becomes prohibitively large. In order to avoid this problem while improving the robustness to measurement uncertainty, Genetic Algorithms were applied for sensor bias detection. The hybrid estimator exhibited excellent performance when at most one sensor was biased. The task of health parameter estimation became more difficult when the bias was of smaller magnitude and was thus less distinguishable from the standard noise level. Since measurement shifts due to health degradations are often small compared to sensor noise, and distinctive health degradations do not necessarily result in distinctive

measurement shifts, it is difficult to obtain one solution with a high level of confidence. This problem was handled by ranking individuals in the GA population set based on their corresponding fitness values. This approach reveals a potential method of reducing the rate of false alarms and missed detections.

There are, however, areas for further improvement. A systematic way of selecting and/or locating sensors for health estimation is desired. Simply increasing the number of sensors for health diagnostics does not guarantee improved estimation performance. Moreover, as the number of sensors increases, the chance of having biases in multiple measurements increases. Another desired improvement is a reduction of the required computing time. A real-time, on-board diagnostic system which can be integrated with a control system is desirable, but difficult to achieve with the proposed architecture. In future work, new approaches that allow improved computing speed without sacrificing reliability will be investigated.

References

- ¹ Simon, D. L., "An Overview of the NASA Aviation Safety Program Propulsion Health Monitoring Element," Paper AIAA-2000-3624, AIAA 36th Joint Propulsion Conference, Huntsville, AL, 2000.
- ² Doel, D. L., "TEMPER - A Gas Path Analysis Tool for Commercial Jet Engines," ASME Journal of Engineering for Gas Turbines and Power, Vol. 116, pp. 82-89, 1994.
- ³ Doel, D. L., "An Assessment of Weighted-Least-Squares-Based Gas Path Analysis," ASME Journal of Engineering for Gas Turbines and Power, Vol. 116, pp. 336-373, 1994.
- ⁴ Volponi, A. J., "Sensor Error Compensation in Engine Performance Diagnostics," ASME Paper 94-GT-58, International Gas Turbine and Aeroengine Congress and Exposition, The Hague, Netherlands, 1994.
- ⁵ Kerr, L. J., Nemec, T. S., and Gallops, G. W., "Real-Time Estimation of Gas Turbine Engine Damage Using a Control Based Kalman Filter Algorithm," ASME Paper 91-GT-216, International Gas Turbine and Aeroengine Congress and Exposition, Orlando, FL, 1991.
- ⁶ Luppold, R. H., Roman, J. R., Gallops, G. W., and Kerr, L. J., "Estimating In-Flight Engine Performance Variations Using Kalman Filter Concepts," Paper AIAA-89-2584, AIAA 25th Joint Propulsion Conference, Monterey, CA, 1989.
- ⁷ DePold, H. R., and Gass, F. D., "The Application of Expert Systems and Neural Networks to Gas Turbine Prognostics and Diagnostics," ASME Journal of Engineering for Gas Turbines and Power, Vol. 121, pp. 607-612, 1999.
- ⁸ Zedda M., and Singh, R., "Fault Diagnosis of a Turbofan Engine Using Neural Networks: A Quantitative Approach," Paper AIAA 98-3602, AIAA 34th Joint Propulsion Conference, Cleveland, Oh, 1998.
- ⁹ Zedda, M., and Singh, R., "Gas Turbine Engine and Sensor Fault Diagnosis Using Optimisation Techniques," Paper AIAA 99-2530, AIAA 35th Joint Propulsion Conference, Los Angeles, CA, 1999.
- ¹⁰ Gulati, A., Zedda, M., and Singh, R., "Gas Turbine Engine and Sensor Multiple Operating Point Analysis Using Optimization Techniques," Paper AIAA 2000-3716, AIAA 36th Joint Propulsion Conference, Huntsville, AL, 2000.
- ¹¹ Urban, L. A., "Gas Path Analysis Applied to Turbine Engine Condition Monitoring," Paper AIAA 72-1082, AIAA 8th Joint Propulsion Specialist Conference, New Orleans, LA, 1972.
- ¹² Adibhatla, S., and Lewis, T. J., "Model-Based Intelligent Digital Engine Control (MoBIDEC)," Paper AIAA-97-3192, AIAA 33rd Joint Propulsion Conference, Seattle, WA, 1997.
- ¹³ Stamatis, A., Mathioudakis, K., Berios, G., and Papailiou, K., "Jet Engine Fault Detection with Differential Gas Path Analysis at Discrete Operating Points," ISABE 89-7133.

| REPORT DOCUMENTATION PAGE | | | Form Approved OMB No. 0704-0188 | |
|--|---|--|---|--|
| Public reporting burden for this collection of information is estimated to average 1 hour per response, including the time for reviewing instructions, searching existing data sources, gathering and maintaining the data needed, and completing and reviewing the collection of information. Send comments regarding this burden estimate or any other aspect of this collection of information, including suggestions for reducing this burden, to Washington Headquarters Services, Directorate for Information Operations and Reports, 1215 Jefferson Davis Highway, Suite 1204, Arlington, VA 22202-4302, and to the Office of Management and Budget, Paperwork Reduction Project (0704-0188), Washington, DC 20503. | | | | |
| 1. AGENCY USE ONLY (Leave blank) | | 2. REPORT DATE July 2001 | | 3. REPORT TYPE AND DATES COVERED Technical Memorandum |
| 4. TITLE AND SUBTITLE A Hybrid Neural Network-Genetic Algorithm Technique for Aircraft Engine Performance Diagnostics | | | 5. FUNDING NUMBERS WU-728-30-20-00 1L161102AH45 | |
| 6. AUTHOR(S) Takahisa Kobayashi and Donald L. Simon | | | | |
| 7. PERFORMING ORGANIZATION NAME(S) AND ADDRESS(ES) National Aeronautics and Space Administration John H. Glenn Research Center Cleveland, Ohio 44135-3191 and U.S. Army Research Laboratory Cleveland, Ohio 44135-3191 | | | 8. PERFORMING ORGANIZATION REPORT NUMBER E-12931 | |
| 9. SPONSORING/MONITORING AGENCY NAME(S) AND ADDRESS(ES) National Aeronautics and Space Administration Washington, DC 20546-0001 and U.S. Army Research Laboratory Adelphi, Maryland 20783-1145 | | | 10. SPONSORING/MONITORING AGENCY REPORT NUMBER NASA TM-2001-211088 ARL-TR-1266 AIAA-2001-3763 | |
| 11. SUPPLEMENTARY NOTES Prepared for the 37th Joint Propulsion Conference and Exhibit cosponsored by the AIAA, ASME, SAE, and ASEE, Salt Lake City, Utah, July 8-11, 2001. Takahisa Kobayashi, QSS Group, Inc., 2000 Aerospace Parkway, Brook Park, Ohio 44142; and Donald L. Simon, U.S. Army Research Laboratory, NASA Glenn Research Center. Responsible person Donald L. Simon, organization code 0300, 216-433-3740. | | | | |
| 12a. DISTRIBUTION/AVAILABILITY STATEMENT Unclassified - Unlimited Subject Category: 07 Available electronically at http://gltrs.grc.nasa.gov/GLTRS This publication is available from the NASA Center for AeroSpace Information, 301-621-0390. | | | 12b. DISTRIBUTION CODE | |
| 13. ABSTRACT (Maximum 200 words) In this paper, a model-based diagnostic method, which utilizes Neural Networks and Genetic Algorithms, is investigated. Neural networks are applied to estimate the engine internal health, and Genetic Algorithms are applied for sensor bias detection and estimation. This hybrid approach takes advantage of the nonlinear estimation capability provided by neural networks while improving the robustness to measurement uncertainty through the application of Genetic Algorithms. The hybrid diagnostic technique also has the ability to rank multiple potential solutions for a given set of anomalous sensor measurements in order to reduce false alarms and missed detections. The performance of the hybrid diagnostic technique is evaluated through some case studies derived from a turbofan engine simulation. The results show this approach is promising for reliable diagnostics of aircraft engines. | | | | |
| 14. SUBJECT TERMS Aircraft engines; Systems health monitoring; Gas turbine engines; Flight safety | | | 15. NUMBER OF PAGES 17 | |
| | | | 16. PRICE CODE | |
| 17. SECURITY CLASSIFICATION OF REPORT Unclassified | 18. SECURITY CLASSIFICATION OF THIS PAGE Unclassified | 19. SECURITY CLASSIFICATION OF ABSTRACT Unclassified | 20. LIMITATION OF ABSTRACT | |